Molecular Biology of the Cell
Vol. 21, 4349–4360, December 15, 2010

A Novel Role of Dma1 in Regulating Forespore Membrane Assembly and Sporulation in Fission Yeast

Wen-zhu Li, Zhi-yong Yu,* Peng-fei Ma,* Yamei Wang, and Quan-wen Jin

Key Laboratory of the Ministry of Education for Cell Biology and Tumor Cell Engineering, School of Life Sciences, Xiamen University, Xiamen 361005, Fujian, China

Submitted February 1, 2010; Revised October 13, 2010; Accepted October 19, 2010
Monitoring Editor: Rong Li

In fission yeast *Schizosaccharomyces pombe*, a diploid mother cell differentiates into an ascus containing four haploid ascospores following meiotic nuclear divisions, through a process called sporulation. Several meiosis-specific proteins of fission yeast have been identified to play essential roles in meiotic progression and sporulation. We report here an unexpected function of mitotic spindle checkpoint protein Dma1 in proper spore formation. Consistent with its function in sporulation, expression of *dma1*$^+$ is up-regulated during meiosis I and II. We showed that Dma1 localizes to the SPB during meiosis and the maintenance of this localization at meiosis II depends on septation initiation network (SIN) scaffold proteins Sid4 and Cdc11. Cells lacking Dma1 display defects associated with sporulation but not nuclear division, leading frequently to formation of asci with fewer spores. Our genetic analyses support the notion that Dma1 functions in parallel with the meiosis-specific Sid2-related protein kinase Slk1/Mug27 and the SIN signaling during sporulation, possibly through regulating proper forespore membrane assembly. Our studies therefore revealed a novel function of Dma1 in regulating sporulation in fission yeast.

INTRODUCTION

Sporulation in the model organism, the fission yeast *Schizosaccharomyces pombe*, is a unique biological process where the plasma membrane of daughter cells is assembled de novo within the mother cell cytoplasm. In recent years, intensive studies in fission yeast have led to a better understanding of the events in sporulation, though our knowledge of the molecular mechanisms that regulate meiosis and sporulation is still limited comparing with the mitotic cell cycle (Shimoda, 2004; Ohtaka *et al*., 2007b). During sporulation, a double-layered membrane called the forespore membrane (FSM) is formed dynamically, and this process is initiated during the second meiotic division. Synthesis of the forespore membrane must be properly coordinated with the second meiotic nuclear division both temporally and spatially, which is essential for accurate distribution of the genome into four haploid spores. A key structure that links these two events is the spindle pole bodies (SPBs), which are the functional equivalent to the centrosomes of animal cells. Thus, the SPB in yeast functions not only to nucleate and organize microtubules, but also to act as a signaling center and a platform that coordinates meiotic cell cycle events.

This article was published online ahead of print in *MBoC in Press* (http://www.molbiolcell.org/cgi/doi/10.1091/mbc.E10–01–0079) on October 27, 2010.

* Z.Y. and P.M. contributed equally to this work.

Address correspondence to: Quan-wen Jin (jinquanwen@xmu.edu.cn).

During meiosis II, at the metaphase-to-anaphase transition, the SPBs are structurally modified as revealed by a transient change in shape from a dot into a crescent (Hagan and Yanagida, 1995). This change results in the formation of a complex multilayered structure called "meiotic plaque," which is essential for spore formation (Tanaka and Hirata, 1982; Hirata and Shimoda, 1994; Ikemoto *et al*., 2000). The inner side of the plaque forms the meiotic spindle, whereas its outer side serves as a platform for assembly of the forespore membrane (Tanaka and Hirata, 1982; Hirata and Shimoda, 1994). After SPB maturation and structural modification, membranous vesicles are targeted to the meiotic outer plaque and promote FSM growth and expansion by vesicle fusion. FSM eventually encapsulates each of the four haploid nuclei and then spore walls are synthesized by the accumulation of wall materials—lipids and polysaccharides—between the inner and outer membranes of the forespore (reviewed in Shimoda, 2004).

Quite a number of genes required for sporulation in fission yeast have been identified and functionally analyzed. The constitutive SPB protein Spo15 is located on the meiotic plaque and plays a critical role in SPB modification and sequential recruitment of a few other sporulation-specific SPB proteins (such as Spo13 and Spo2) to assist SPB maturation (Ikemoto *et al*., 2000; Nakase *et al*., 2008). When SPB modification is blocked by mutation of Spo15, sporulation is totally abolished (Ikemoto *et al*., 2000; Nakase *et al*., 2008). After SPB maturation, the coiled-coil–containing protein Spo3 and the syntaxin-related protein Psy1 participate in SPB targeting of secretory vesicles (Nakamura *et al*., 2001). FSM outgrowth is initiated at each of the modified SPBs and subsequently proceeds toward the midspindle region with Meu14 as the major component of a ring structure at the leading edge (Okuzaki *et al*., 2003; Shimoda, 2004). After completion of spore membrane assembly, the spore wall is assembled by the combined action of enzymes, such as Ags1/Mok1, Bgs2 and Chs1 (Hochstenbach *et al*., 1998; Arel-

lano *et al.*, 2000; Liu *et al.*, 2000; Martin *et al.*, 2000; Vos *et al.*, 2007).

At the end of the vegetative cell cycle in fission yeast, a signaling cascade termed the septation initiation network (SIN) is required to regulate the onset of cytokinesis and septum formation (reviewed in McCollum and Gould, 2001; Guertin *et al.*, 2002a; Krapp and Simanis, 2008). The SIN pathway includes a small GTPase (Spg1), three protein kinases (Cdc7, Sid1, and Sid2) and two scaffold proteins (Cdc11 and Sid4). All the members of the SIN localize to the SPBs and are thought to coordinate cytokinesis with completion of chromosome segregation (reviewed in McCollum and Gould, 2001; Guertin *et al.*, 2002a; Krapp and Simanis, 2008). Very recent studies have shown that the SIN components also localize to the SPBs during meiosis and play an important role in FSM assembly (Krapp *et al.*, 2006). The defects in FSM assembly have been correlated with improper localization of the t-SNARE Psy1 in some SIN mutants, however the detailed mechanism linking the SIN and FSM assembly remains unclear (Krapp *et al.*, 2006). It has been recently shown that a meiosis-specific Sid2-like kinase Slk1/Mug27 is expressed specifically during meiosis and localizes to the SPBs during meiosis I and II in an SIN-dependent manner (Ohtaka *et al.*, 2008; Perez-Hidalgo *et al.*, 2008; Yan *et al.*, 2008). Examination on the phenotypes during sporulation in *slk1*Δ cells suggested that Slk1/Mug27, together with Sid2, plays a role in forespore membrane assembly by facilitating recruitment of components of the secretory apparatus, such as Psy1, to allow FSM expansion (Ohtaka *et al.*, 2008; Perez-Hidalgo *et al.*, 2008; Yan *et al.*, 2008). These studies thereby provided a novel link between the SIN and vesicle trafficking during cytokinesis.

An SPB-localized protein, Dma1, has been identified as a negative regulator of mitotic exit and cytokinesis in late mitosis (Murone and Simanis, 1996; Guertin *et al.*, 2002b). In mitotic cells, Dma1 localizes at the SPBs through interaction with Sid4, which is a scaffold protein required for recruiting SIN components to the SPB (Chang and Gould, 2000; Guertin *et al.*, 2002a; Guertin *et al.*, 2002b). So far, nothing is known about the function of Dma1 during meiosis. Whether Dma1 negatively regulates SIN components in meiosis as it does in mitotic exit and cytokinesis remains an open question. According to the *S. pombe* genome-wide transcriptome analysis, expression of *dma1*$^+$ is clearly up-regulated during meiosis (Mata *et al.*, 2002), suggesting that Dma1 may be involved in regulation of meiotic events. Here we report that indeed Dma1 is also localized to the SPB during meiosis and plays a pivotal role in FSM formation and sporulation. Our results suggest that Dma1 fulfills its function during sporulation possibly through cooperating with the SIN and meiosis-specific kinase Slk1/Mug27.

MATERIALS AND METHODS

Yeast Strains, Media, and Culture Conditions

Schizosaccharomyces pombe strains used in this study are listed in Table 1. Yeast strains were constructed by either random spore method or by tetrad analysis. Yeast cells were grown on YES medium or minimal media with appropriate supplements (Moreno *et al.*, 1991). Solid malt extract (ME) medium or synthetic Edinburgh minimal medium without nitrogen (EMM-N) was used for mating and sporulation. Homothallic yeast strains were induced to enter meiosis and sporulation on ME for 24 h at 25°C or for 14 h at 30°C. For *cdc11*-123, *sid4*-A1, and *sid2-250* mutants, sporulation was induced on ME at 25°C, 28°C, 30°C, or 35°C and processed for staining (DAPI or Hoechst) or imaging experiments as the case may be. The induction of synchronous meiosis and meiotic time course experiments using *pat1-114* mutants were performed as described previously (Loidl and Lorenz, 2009). Growth temperatures were 25°C (permissive) for temperature-sensitive strains, and 30°C for all other strains.

Construction of Gene Replacement Strains Carrying *dma1*$^{\Delta FHA}$ or *dma1*$^{\Delta RF}$

The fragments containing *dma1*$^{\Delta FHA}$ (344-804 bp) or *dma1*$^{\Delta RF}$ (1-572 bp) flanked by ~500 bp *dma1*$^+$ 5′UTR and ~500 bp *dma1*$^+$ 3′UTR regions were amplified by fusion PCRs using primers containing *Pst*I and *Sal*I sites. Primers used were: dma1-5′UTR(500 bp)-*Sal*I-F: 5′-GCGCGTCGACCTGTGTGCAATTTACTTG-3′; dma1-ΔRF-3′R: 5′-CTGAAAATAACAGTTTATTCCGGAGGACCCGATTC-3′; dma1-3′UTR-5′F: 5′-CCTCCGGAATAAACTGTTATTTTCAGTATGG-3′; dma1-3′UTR(500bp)-*Pst*I-R: 5′-CGTTCTGCAGGACTCTCAGAAGAACAAC-3′; dma1-5′UTR-3′R: 5′-GGTGATAAACCATTTTTTGGAAAGAAAAGC-3′; dma1-ΔFHA-5′F: 5′-CTTTCCAAAAAATGGTTTATCACCGCCGTC-3′. PCR products were digested with *Pst*I and *Sal*I and cloned into a similarly digested pBluescript-SK vector. To generate strains carrying integrated version of *dma1*$^{\Delta FHA}$ or *dma1*$^{\Delta RF}$ under the native *dma1*$^+$ promoter, plasmids pBluescript-SK-*dma1*$^{\Delta FHA}$ and pBluescript-SK-*dma1*$^{\Delta RF}$ were linearized with *Pst*I and transformed into *dma1*Δ*::ura4*$^+$ cells. Correct integrations into the *S. pombe dma1*$^+$ locus by homologous recombination were selected by failure to grow on EMM-uracil plates (Ura- colonies) and were subsequently confirmed on FOA plates and by PCR analysis.

Construction of Strain Overexpressing Slk1 under nmt1 Promoter

The coding region of *slk1*$^+$ gene was first amplified by PCR using primers containing *Xma*I sites. Primers used were: slk1-*Xma*I-F: 5′-TCCCCCGGGGTATGGACCTACTGGGCC-3′ and slk1-*Xma*I-R: 5′-TCCCCCGGGTTAGAGCAAAAATTCATAC-3′. PCR product was digested with *Xma*I and cloned into a similarly digested pREP1-GFP(N) vector. The fragment containing *nmt1* promoter, GFP coding region, *slk1*$^+$ gene, and *nmt1* terminator was cut out by digestion with *Pst*I and *Sac*I and cloned into pJK148 vector. The resultant plasmid was linearized by digestion with *Bsu36*I (which cuts in the coding region of the *leu1*$^+$ gene) and transformed into *leu1-32* strain. Correct integrations into the *S. pombe leu1*$^+$ locus by homologous recombination were selected by growth on EMM-leu plates and were subsequently confirmed by PCR analysis.

RNA and Protein Methods

Total RNA was isolated from cells collected at each time points of the meiotic time course by using the TriPure Isolation Reagent (Roche, Indianapolis, IN) and following manufacturer's instructions. RT was performed with PrimeScript RT reagent Kit (Takara Bio, Shiga, Japan) at 37°C for 15 min followed by treatment at 85°C for 5 s. Quantitative real-time PCR was performed on a Rotor-Gene 3000A instrument using SYBR Premix Ex Taq (Takara). Relative RNA levels were calculated from Δ*CT* values and normalized to *act1*$^+$ RNA levels. The melting curve in each individual measurement was monitored to guard against nonspecific amplification. Primer pairs to detect *dma1*$^+$ and *act1*$^+$ transcripts were as follows: dma1-F-527: 5′-GCAAGAACTGGTGTTATGCGG-3′ and dma1-R-781: 5′-CCGTTGCATTTCGTAGAAGG-3′ (amplifying a 254bp fragment); act1-F: 5′-GTATGCCTCTGGTCGTACCAC-3′ and act1-R: 5′-CAATTTCACGTTCGGCGGTAG-3′ (amplifying a 200bp fragment).

Total protein extracts were made using the 8M urea extraction protocol (Masai *et al.*, 1995). Protein extracts were run on 8–10% SDS-PAGE gels and transferred to nitrocellulose membranes (GE, Munich, Germany). For detection, mouse monoclonal anti-GFP (Roche or Santa Cruz Biotechnology, Santa Cruz, CA) or anti-myc (Roche) was used as the primary antibody (1:1000 dilution). Tubulin was detected using mouse monoclonal anti-TAT1 antibodies (1:3000 dilution). Goat anti-mouse conjugated to horseradish peroxidase (Pierce, Rockford, IL) was used as the secondary antibody at 1:10,000 dilution. Membranes were developed with Supersignal (Pierce) or ECL western blotting reagents (GE).

For coimmunoprecipitation experiments, whole-cell lysates were prepared in NP-40 buffer (6 mM Na_2HPO_4, 4 mM NaH_2PO_4, 1% NP-40, 150 mM NaCl, 2 mM EDTA, 50 mM NaF, 0.1 mM Na_3VO_4) and lysates were subjected to immunoprecipitation with anti-GFP (3E6; Molecular Probes, Eugene, OR) antibodies and Western blot analyses with anti-GFP or anti-Myc (9E10, Roche) antibodies were performed as previously described (Guertin *et al.*, 2002b).

Spore Viability

Dissected spores' viability was determined as described previously (Ohtaka *et al.*, 2007a; Ohtaka *et al.*, 2008). Briefly, *h*^{90} haploid wild-type or *dma1*Δ strains were grown on YE plates at 30°C. Cells were mated and sporulated on ME plates at 30°C for 3–4 d. The spores from 4-spore asci were separated on YE agar plates by using a micromanipulator (Schuett Biotec, Germany). The plates were incubated at 30°C for 4–5 d, after which spore viability was calculated.

Microscopy

GFP or RFP-fusion proteins were observed in cells after fixation with cold methanol or in live cells. For DAPI (4′, 6-diamidino-2-phenylindole, Sigma, St. Louis, MO) staining of nuclei, cells were fixed with cold methanol, washed in PBS and resuspended in PBS plus 1 μg/ml DAPI. Nucleus staining of live cells was performed with Hoechst 33342 (Sigma) at 1–2 μg/ml in EMM or PBS. Photomicrographs were obtained using a Nikon 80i fluorescence micro-

Table 1. Yeast strains used in this study

Name	Genotype	Source
JY1	*h⁻ ade6-210 leu1-32 ura4-D18*	Lab stock
JY2	*h⁺ ade6-210 leu1-32 ura4-D18*	Lab stock
JY78	*h⁻ dma1::ura4⁺ ade6-21x leu1-32 ura4-D18*	Lab stock
JY92	*h⁺ dma1::ura4⁺ ade6-21x leu1-32 ura4-D18*	Lab stock
JY709	*h⁹⁰ spo3-GFP>>LEU2 leu1-32*	YGRC
JY760	*h⁹⁰ spo3-GFP>>LEU2 dma1::kan^R ade6-210 leu1-32 ura4-D18*	This study
JY810	*h⁺/h⁻ pat1-114/pat1-114 dma1-GFP::kan^R/dma1-GFP::kan^R ade6-210/ade6-216 leu1-32/leu1-32 ura4-D18/ura4-D18*	This study
JY812	*h⁺/h⁻ pat1-114/pat1-114 dma1::ura4⁺/dma1::ura4⁺ ade6-210/ade6-216 leu1-32/leu1-32 ura4-D18/ura4-D18*	This study
JY904	*h⁹⁰ spo15-GFP::leu1⁺ sad1-GFP>>kan^R ade6-21x leu1-32 ura4-D18*	This study
JY903	*h⁹⁰ spo15-GFP::leu1⁺ sad1-GFP>>kan^R dma1::ura4⁺ ade6-21x leu1-32 ura4-D18*	This study
JY909	*h⁹⁰ sid4-GFP::kan^R ade6-21x leu1-32 ura4-D18*	This study
JY887	*h⁹⁰ sid4-GFP::kan^R dma1::ura4⁺ ade6-21x leu1-32 ura4-D18*	This study
JY911	*h⁹⁰ cut12-EGFP::ura4⁺ ade6-21x leu1-32 ura4-D18*	This study
JY888	*h⁹⁰ cut12-EGFP::ura4⁺ dma1::kan^R ade6-21x leu1-32 ura4-D18*	This study
JY1200	*h⁹⁰ slk1/mug27::ura4⁺ ade6-210 leu1-32 ura4-D18*	M. Balasubramanian
JY1286	*h⁹⁰ slk1/mug27::ura4⁺ dma1::kan^R ade6-210 leu1-32 ura4-D18*	This study
JY1202	*h⁹⁰ slk1/mug27-GFP::ura4⁺ ade6-210 leu1-32 ura4-D18*	M. Balasubramanian
JY1256	*h⁹⁰ slk1/mug27-GFP::ura4⁺ dma1::kan^R ade6-210 leu1-32 ura4-D18*	This study
JY1206	*h⁻ pat1-114 slk1/mug27::[slk1/mug27-9myc-3′UTR-LEU2] ade6-210 leu1-32 ura4-D18*	YGRC
JY1347	*h⁻ pat1-114 slk1/mug27::[slk1/mug27-9myc-3′UTR-LEU2] dma1-GFP::kan^R ade6-210 leu1-32 ura4-D18*	This study
JY1293	*h⁻ pat1-114 slk1/mug27::[slk1/mug27-9myc-3′UTR-LEU2] dma1::ura4⁺ ade6-210 leu1-32 ura4-D18*	This study
JY1558	*h⁹⁰ plo1-24C ade6-21x leu1-32 ura4-D18*	This study
JY1557	*h⁹⁰ dma1::ura4⁺ plo1-24C ade6-21x leu1-32 ura4-D18*	This study
JY1252	*h⁹⁰ sid4-A1 ade6-21x leu1-32 ura4-D18*	This study
JY1232	*h⁹⁰ sid4-A1 dma1::ura4⁺ ade6-21x leu1-32 ura4-D18*	This study
JY1253	*h⁹⁰ sid4-GFP::kan^R cdc11-123 ade6-21x leu1-32 ura4-D18*	This study
JY1233	*h⁹⁰ sid4-GFP::kan^R cdc11-123 dma1::ura4⁺ ade6-21x leu1-32 ura4-D18*	This study
JY1596	*h⁹⁰ spg1-106 ade6-21x leu1-32 ura4-D18*	This study
JY1586	*h⁹⁰ dma1::ura4⁺ spg1-106 ade6-21x leu1-32 ura4-D18*	This study
JY1585	*h⁹⁰ cdc7-24 ade6-21x leu1-32 ura4-D18*	This study
JY1595	*h⁹⁰ dma1::ura4⁺ cdc7-24 ade6-21x leu1-32 ura4-D18*	This study
JY1559	*h⁹⁰ sid1-239 ade6-21x leu1-32 ura4-D18*	This study
JY1597	*h⁹⁰ dma1::ura4⁺ sid1-239 ade6-21x leu1-32 ura4-D18*	This study
JY1234	*h⁹⁰ sid2-250 ade6-21x leu1-32 ura4-D18*	This study
JY1235	*h⁹⁰ sid2-250 dma1::ura4⁺ ade6-21x leu1-32 ura4-D18*	This study
JY1598	*h⁹⁰ mob1-1 ade6-21x leu1-32 ura4-D18*	This study
JY1599	*h⁹⁰ mob1-1 dma1::ura4⁺ ade6-21x leu1-32 ura4-D18*	This study
JY1229	*h⁹⁰ dma1-GFP::kan^R spo15::ura4⁺ ade6-21x leu1-32 ura4-D18*	This study
JY1258	*h⁹⁰ dma1-GFP::kan^R spo3::ura4⁺ ade6-216 leu1-32 ura4-D18*	This study
JY1260	*h⁹⁰ dma1-GFP::kan^R sid4-A1 ade6-21x leu1-32 ura4-D18*	This study
JY1262	*h⁹⁰ dma1-GFP::kan^R cdc11-123 ade6-210 leu1-32 ura4-D18*	This study
JY1276	*h⁹⁰ dma1-GFP::kan^R sad1-RFP::kan^R ade6-21x leu1-32 ura4-D18*	This study
JY1248	*h⁹⁰ leu1⁺>>psy1(p)GFP-psy1 GFP-atb2⁺-kan^R ade6-21x ura4-D18*	This study
JY993	*h⁹⁰ leu1⁺>>psy1(p)GFP-psy1 GFP-atb2⁺-kan^R dma1::ura4⁺ ade6-216 ura4-D18*	This study
JY1278	*h⁹⁰ sid2-GFP::ura4⁺ ade6-210 leu1-32 ura4-D18*	This study
JY1244	*h⁹⁰ sid2-GFP::ura4⁺ dma1::kan^R ade6-210 leu1-32 ura4-D18*	This study
JY1280	*h⁹⁰ cdc11-GFP::kan^R ade6-21x leu1-32 ura4-D18*	This study
JY1246	*h⁹⁰ cdc11-GFP::kan^R dma1::ura4⁺ ade6-21x leu1-32 ura4-D18*	This study
JY1203	*h⁻ pat1-114 slk1/mug27::[slk1/mug27-GFP-3′UTR-LEU2] ade6-216 leu1-32 ura4-D18*	YGRC
JY1356	*h⁺ pat1-114 slk1/mug27::[slk1/mug27-GFP-3′UTR-LEU2] ade6-21x leu1-32 ura4-D18*	This study
JY1294	*h⁺ pat1-114 slk1/mug27::[slk1/mug27-GFP-3′UTR-LEU2] dma1::ura4⁺ ade6-216 leu1-32 ura4-D18*	This study
JY1295	*h⁻ pat1-114 slk1/mug27::[slk1/mug27-GFP-3′UTR-LEU2] dma1::ura4⁺ ade6-216 leu1-32 ura4-D18*	This study
JY1296	*h⁹⁰ leu1⁺>>psy1(p)GFP-psy1 dma1^ΔFHA ade6-216 ura4-D18*	This study
JY1298	*h⁹⁰ leu1⁺>>psy1(p)GFP-psy1 dma1^ΔRF ade6-216 ura4-D18*	This study
JY1329	*h⁻ pat1-114 dma1-GFP-kan^R ade6-216*	This study
JY1339	*h⁻ pat1-114 dma1::ura4⁺ ade6-216*	This study
JY111	*h⁺ cen2>>lacO-kan^R-ura4⁺ his7⁺>>GFP-lacI-NLS leu1-32 lys1 ura4-D18 ade6-M216*	Y. Watanabe
JY470	*h⁺ dma1Δ::ura4⁺ cen2>>lacO-kan^R-ura4⁺ his7⁺>>GFP-lacI-NLS ura4-D18 leu1-32 ade6-21x lys1*	This study
JY1477	*h⁹⁰ nmt1-GFP-slk1::leu1⁺ slk1-GFP::ura4⁺ ade6-210 leu1-32 ura4-D18*	This study
JY1563	*h⁹⁰ nmt1-GFP-slk1::leu1⁺ dma1::kan^R ade6-210 leu1-32 ura4-D18*	This study

scope coupled to a cooled CCD camera (Hamamatsu, ORCA-ER) and image processing and analysis was carried out using Element software (Nikon) and Adobe Photoshop. For time-lapse microscopy, homothallic wild-type or *dma1*Δ cells carrying GFP-Psy1 and GFP-Atb2 were first induced to enter meiosis on solid ME plates for 10–12 h. Live cells were then spotted on a glass slide containing 2% agar pad with EMM-N at room temperature (~25°C). Images were acquired every 3–10 min (with a 400–600 ms exposure time).

RESULTS

Dma1 Expression Is Significantly Up-Regulated during Meiosis

According to previously published microarray expression data, *dma1*$^+$ mRNA is expressed during meiotic prophase and peaked between meiosis I and meiosis II (Mata *et al.*, 2002). To more accurately examine the expression of the *dma1*$^+$ at the mRNA and protein levels during meiosis, we used the haploid *dma1*$^+$-GFP strain, which expresses Dma1 protein tagged with the GFP epitope at its C-terminal end (Guertin *et al.*, 2002b). To obtain synchronous meiosis, we used the *pat1-114* temperature-sensitive strain, which enters meiosis in a highly synchronous manner when it is shifted to the restrictive temperature (Iino and Yamamoto, 1985). The cell lysates from a time course were subjected to total RNA isolation or protein extraction and subsequent quantitative RT-PCR (qRT-PCR) or immunoblot analysis using the anti-GFP antibodies. These analyses revealed that *dma1*$^+$ indeed displayed meiosis-specific up-regulation of transcription, its mRNA level began to increase during prophase and peaked at ~4.5–5 h after the induction of meiosis (Figure 1B). These data are consistent with the microarray expression data (Mata *et al.*, 2002). In parallel, Dma1 protein levels peaked at ~5.5 h and started to decrease at the end of the second meiotic nuclear division (Figure 1C).

Dma1 Is Localized at the Spindle Pole Body during Meiosis and Maintenance of this Localization at Meiosis II Depends on SIN Scaffold Proteins

In mitosis, Dma1 exhibits distinct localization at the SPBs and cell division site from metaphase to anaphase, a pattern similar to some of the SIN components (Guertin *et al.*, 2002b). To gain insight into the cellular role of Dma1 in meiosis, the localization of this protein was analyzed. Dma1-GFP localization was examined in homothallic (h^{90}) cells after induction of meiosis by nitrogen starvation. The SPB marker Sad1 tagged with RFP (RFP-Sad1) was used to monitor cell cycle progression. As shown in Figure 2A, Dma1-GFP was first observed as a dot-like signal at horsetail stage, and during meiosis I and II Dma1-GFP was visible as one, two, or four foci, which were always colocalized with the RFP-Sad1 signals. This colocalization pattern of Dma1 and Sad1 suggested that Dma1 localized to the SPB in meiotic cells similarly to SIN components (Krapp *et al.*, 2006). As sporulation commenced, Dma1-GFP gradually disappeared from the four SPBs, and it showed slight accumulation in the cytoplasm of asci (Figure 2A).

In mitosis, core components of the fission yeast SIN signaling are anchored to the outer plaque of the SPB by Cdc11 and Sid4 (Krapp *et al.*, 2001), and Dma1 is recruited to SPB through its interaction with Sid4 (Guertin *et al.*, 2002b). We wondered whether Dma1's localization to SPB during meiosis and sporulation also requires SIN proteins. To test this possibility, Dma1-GFP localization was examined in temperature-sensitive homothallic *cdc11-123* and *sid4-A1* strains after they were induced into meiosis and sporulation at permissive (25°C) and nonpermissive (28°C for *sid4-A1* and 35°C for *cdc11-123*) temperatures. We found that Dma1-GFP localized normally at SPBs from metaphase I to metaphase II in these mutants at nonpermissive temperatures (Figure 2, B and C, and data not shown). At anaphase II, however, many of the Dma1-GFP signals did not accumulate at SPBs (Figure 2, B and C). These observations suggested that retention of Dma1 localization to SPBs during meiosis II and sporulation depends on the SIN scaffold proteins Cdc11 and Sid4, although the initial recruitment is independent of these two proteins. This pattern of localization dependency is reminiscent of the meiosis-specific kinase Slk1/Mug27, whose stable localization at SPB in meiotic anaphase II also requires Cdc11 and Sid4 (Yan *et al.*, 2008). Furthermore, similarly to Slk1/Mug27 (Yan *et al.*, 2008), Dma1 does not require Spo15 and Spo3 for its proper maintenance at SPBs (Fig. S1).

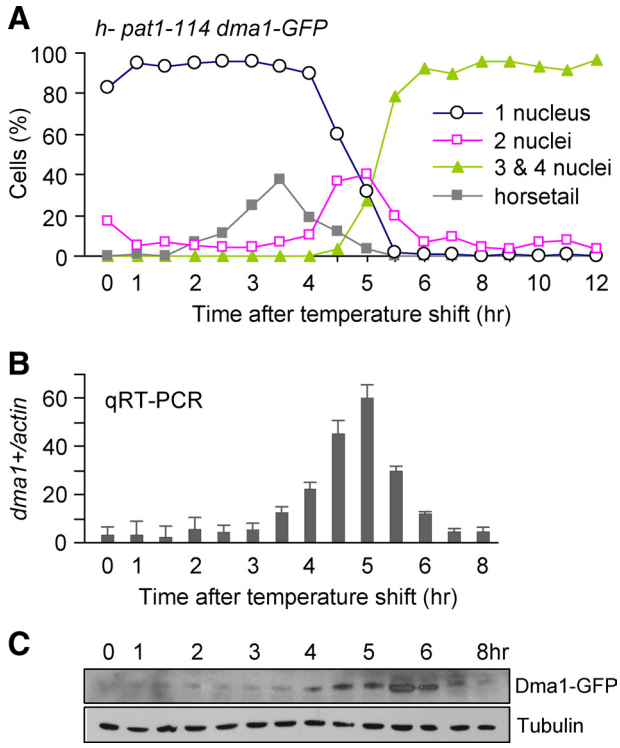

Figure 1. *dma1*$^+$ expression is up-regulated during meiosis I and II. Haploid strain h^- *pat1-114 dma1-GFP* was induced to enter synchronous meiosis by shift from 25°C in EMM-N to 34°C in EMM+N as described (Kitajima *et al.*, 2003a; Loidl and Lorenz, 2009) and cells were sampled at each indicated time point. Meiotic nuclear division (A), the mRNA level of *dma1*$^+$ (B), and the protein level of Dma1 (C) throughout the time course were examined. (A) The progression of meiosis was monitored by DAPI staining after temperature shift. Percentages of cells with one nucleus, two nuclei, and three to four nuclei are shown. Cells undergoing horsetail stage were separately counted. At least 200 cells were counted for each time point. (B) Total RNA was extracted at the indicated time points. Samples were processed with reverse transcription, and the mRNA level of *dma1*$^+$ was analyzed by quantitative real-time PCR (qRT-PCR) using primers to amplify part of *dma1*$^+$. Average values from three experiments were normalized to *act1*$^+$ transcript levels and presented as histograms. Error bars indicate standard deviations. (C) Western blot analysis of the protein level of Dma1 during the synchronous meiosis using anti-GFP antibodies. Tubulin levels are shown as a loading control.

Dma1 Is Not Required for Meiotic Progression and Chromosome Segregation, but Is Required for Proper Spore Formation

Because Dma1 expression was significantly up-regulated and it localized at SPBs during meiosis (Figures 1 and 2), we investigated possible function(s) of this protein in meiosis. To analyze meiotic cell cycle progression in the *dma1*Δ mutant, we induced synchronous meiosis in haploid *pat1-114*

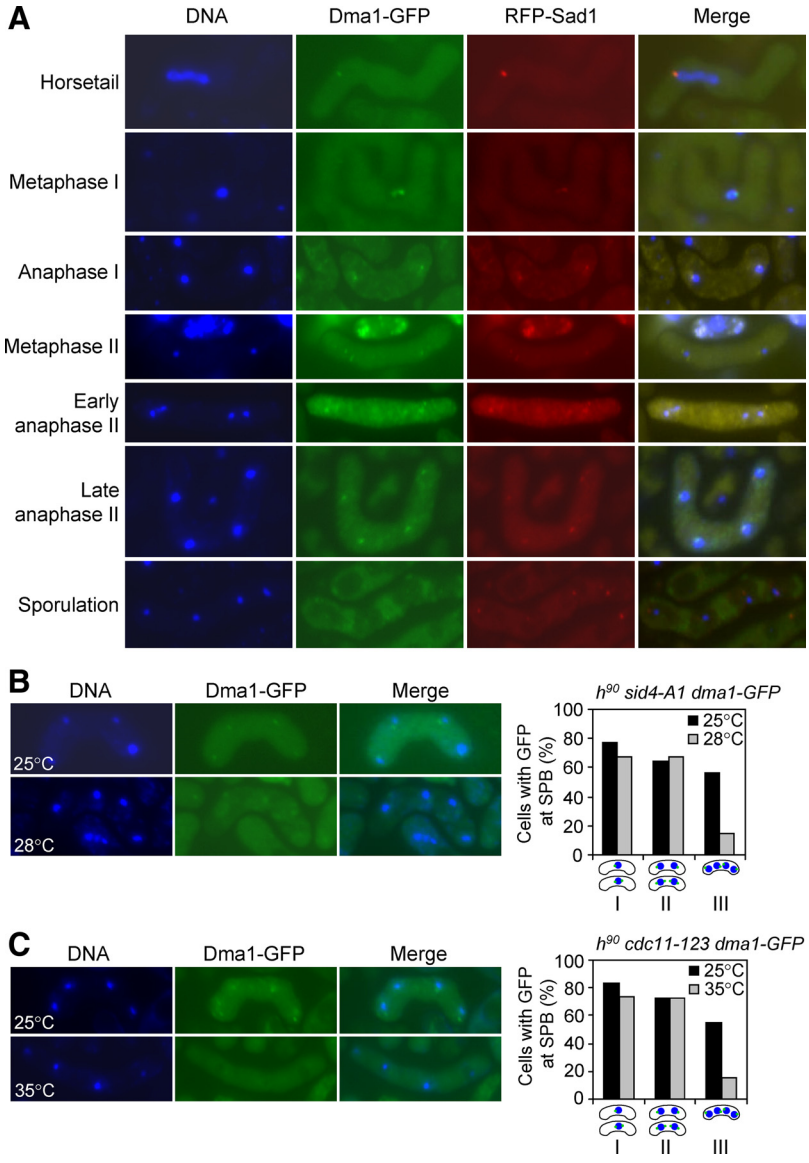

Figure 2. Dma1 is localized at the spindle pole body during meiosis. (A) Dma1-GFP subcellular localization during meiosis relative to RFP-Sad1 was observed by fluorescence microscopy. The *dma1*$^{+}$-*GFP RFP-sad1*$^{+}$ strain was induced to enter meiosis by nitrogen starvation at 30°C. Ten to 20 h later, the cells were collected and stained with Hoechst 33342 to visualize the DNA (blue). The GFP signal is in green, and the RFP signal is in red. (B and C) Dependency of Dma1 at SPB on Sid4 and Cdc11 at meiosis II. Homothallic *sid4-A1* and *cdc11-123* single mutants carrying Dma1-GFP were induced into meiosis on ME plate at 25°C (for both mutants), 28°C (for *sid4-A1* mutant), or 35°C (for *cdc11-123* mutant) for at least 20–24 h. Then the cells of different stages of meiosis were collected and stained with Hoechst 33342. Examples of anaphase II cells are shown. The bar graphs were drawn by determining the Dma1-GFP localization in *sid4-A1* or *cdc11-123* cells and then plotting the frequencies of indicated patterns. At least 20 cells were counted for each category in each strain.

strains. As shown in Figure 3A, after temperature shift *dma1*Δ cells proceeded through meiotic nuclear divisions with kinetics identical to that of the wild-type (as compared with Figure 1A). During the first and second meiotic divisions, chromatin segregation appeared almost normal, as revealed by visualization of cen2-GFP (Kitajima *et al.*, 2003b) (Supplemental Figure S2). However, we noticed that in the absence of *dma1*$^{+}$, the initiation of spore formation was delayed for ~2 h compared with wild-type cells, and also the efficiency of spore formation was dramatically dropped with only ~60% of cells containing spores (Figure 3B). Therefore, we concluded that Dma1 is not essential for progression through the stages of meiosis before spore formation.

In the course of the synchronized meiosis experiment described above, we noticed that *dma1*Δ cells gave rise to large number of abnormal spores (data not shown). Therefore, we next undertook a more detailed examination of the defects in spore formation in *dma1*Δ cells. Heterothallic (*h*$^{+}$ and *h*$^{-}$) or homothallic (*h*^{90}) wild-type cells placed under nitrogen-limiting conditions underwent mating followed by meiosis and sporulation, leading to the formation of four-spored asci (Figure 4A). In contrast, abnormalities related to sporulation were observed when *dma1*Δ cells were placed under the same nitrogen-limiting conditions (Figure 4A). Quantitative analyses revealed that a significant fraction (~75–80%) of *dma1*Δ asci contained one, two, or three, instead of four, spores, indicating incomplete spore formation within these asci (Figure 4B). This was also true for diploid *dma1*Δ cells when they were induced to undergo meiosis and sporulation (Figure 4, A and B). We found the negative effect of *dma1*Δ on spore formation was recessive, as we observed almost normal spore formation when a wild-type haploid strain mated with a *dma1*Δ haploid (Figure 4A).

The spore viability of four-spore asci was analyzed by tetrad dissection and random spore analysis, and we observed normal-looking spores produced by mated *dma1*Δ cells showed slightly reduced germination efficiency compared with wild-type cells (Figure 4C and data not shown). This indicated although some mated *dma1*Δ cells managed to form four spores, a portion of the spores could not germinate to form colonies, presumably because of defective FSM and spore wall assembly (see below).

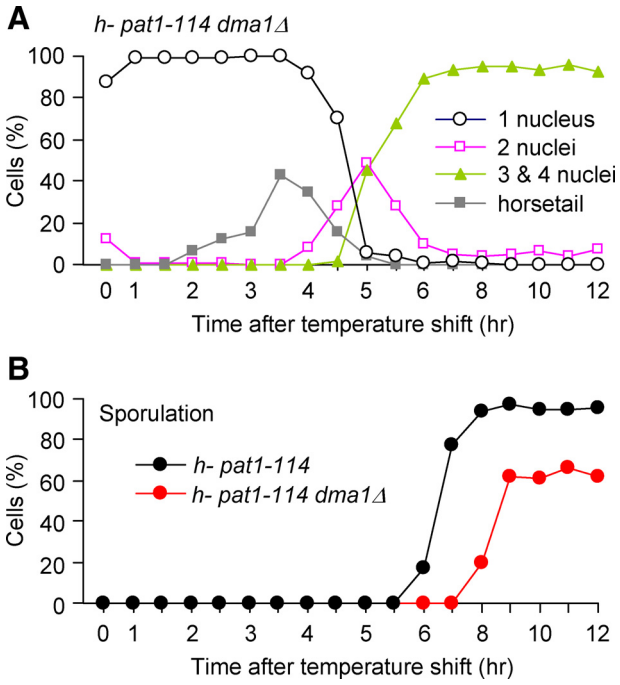

Figure 3. Meiotic progression is normal but spore formation is delayed in *dma1*Δ cells. (A) Profiles of the meiotic progression in *h*$^{-}$ *pat1-114 dma1*Δ (strain JY1339) haploid cells. The progression of meiosis was monitored by DAPI staining after temperature shift as in Figure 1A. Percentages of cells with one nucleus, two nuclei, and three to four nuclei are shown. Cells undergoing horsetail stage were separately counted. At least 200 cells were counted at each time point. (B) Spore formation was monitored by DIC microscope in the same time course experiments shown in A and Figure 1A. At least 200 cells were counted at each time point.

Dma1 contains two recognized domains: an N-terminal FHA domain and a C-terminal RING-H2 (RH2) finger (RF) (Murone and Simanis, 1996; Guertin *et al*., 2002b). To determine which domain is more specifically required for the role Dma1 plays in spore formation, we generated partial deletion mutants (Dma1$^{\Delta FHA}$ or Dma1$^{\Delta RF}$) in which either FHA or RF domain was deleted in the genome (Figure 4D). Examination of spore formation in these mutant cells indicated that absence of either domain led to increase of asci containing fewer than four spores similar to *dma1*Δ cells (Figure 4E). These data showed that both FHA and RF domains are required for the function of Dma1 in regulating sporulation.

Spore Membrane Assembly Is Aberrant in dma1Δ *Cells, But Meiotic Plaque Assembly Is Normal*

To understand the molecular basis of the spore formation defects in *dma1*Δ cells, we examined the localization of several proteins that participate at distinct steps during sporulation. The formation of the crescent-shaped meiotic outer plaque during SPB modifications depends on the SPB-associated protein Spo15 (Ikemoto *et al*., 2000). Because Dma1 is already present at the SPB from the early stage of FSM assembly, we decided to test whether the modification of the SPB is impaired in *dma1*Δ cells. We found that the localization of Spo15 and the assembly of the Spo15 crescents were unaffected in *dma1*Δ cells (Supplemental Figure S3). Our observation of the SPB protein Cut12 by using a chromosomally GFP-tagged allele (*cut12-GFP*) (Bridge *et al*., 1998) also revealed the presence of the typical crescent-shaped SPBs in *dma1*Δ cells (Supplemental Figure S3). These data indicated that Dma1 is not required for the meiosis-specific modification of the SPB.

It is known that after SPB maturation, the syntaxin-related protein Psy1 participates in the process of FSM development by promoting targeting of membranous vesicles to the meiotic outer plaque (Nakamura *et al*., 2001; Shimoda, 2004). So we next investigated the localization and behavior of Psy1 in wild-type and *dma1*Δ cells using strains that simultaneously express GFP-Psy1 and GFP-Atb2, which labeled FSM and tubulin respectively. Similar to what we observed in wild-type cells, GFP-Psy1 in *dma1*Δ cells appeared as two pairs of bright crescent near the SPBs at metaphase II and formed two pairs of cup-like structures facing each other in the asci (Figure 5A). However, we found small-sized GFP-Psy1 aggregates without hollow internal space in many *dma1*Δ asci (Figure 5, A and B). These aggregates were often observed in the same asci as normal-looking sphere-like structures (Figure 5, A and B), suggesting that they could have been derived from collapsed or shrunk sphere-like structures. Other defects in GFP-Psy1 localization in *dma1*Δ asci included the following: a small proportion of asci containing only three GFP-Psy1 aggregates or spheres, as well as many asci (almost 40%) containing more than four (up to 8) discernable GFP-Psy1 aggregates or spheres (Figure 5, A–C). To investigate whether the normal-looking GFP-Psy1 spheres could result in normal spore formation, we counted the asci with one, two, three, or four normal-looking GFP-Psy1 spheres. Interestingly, the frequencies of each class corresponded very well to the frequencies of asci containing same number of spores (compare Figure 5D with Figure 4B). This suggested that once the FSM formed normally, the relatively normal spore development was followed.

To further examine in detail how the FSM formation defects is generated in live *dma1*Δ cells, we compared the behavior of GFP-Psy1 by time-lapse microscopy in asci from wild-type and *dma1*Δ cells after two metaphase II spindles were fully assembled (as indicated by GFP-Atb2). As previously reported (Nakamura *et al*., 2008; Yan *et al*., 2008), GFP-Psy1 in wild-type cells progressively formed crescent-shaped structures besides the SPBs at metaphase II, later expanded as four cup-like structures, and eventually became four round mature structures in the asci (Figure 6A). However, we observed several types of defects in FSM development in *dma1*Δ cells (Figure 6B). These defects roughly fell into three classes: (1) initially FSM formation was normal and appeared as sphere structure, but subsequently it became smaller or collapsed (asterisks in Figure 6B); (2) crescent-shaped structures did not properly develop into cup-like structures (open arrows in Figure 6B); and (3) crescent-shaped structures broke into multiple GFP-Psy1-contaning structures which could not develop into round mature FSMs (arrows in Figure 6B).

Collectively, our data suggested that the inability of *dma1*Δ cells to form proper ascospores might result from defective FSM development at different stages, such as failed transition from crescent structure to cup-like structure, abnormal further expansion of the spore membrane, or the failed maintenance of the round structure at the spore periphery.

Negative Genetic Interactions between spo3-GFP *and* dma1Δ *Mutant*

Because we found the defects of forespore membrane development in *dma1*Δ cells, we were interested in knowing the effect of compromised FSM proteins on sporulation in *dma1*Δ. Spo3 is a coiled-coil–containing protein required for

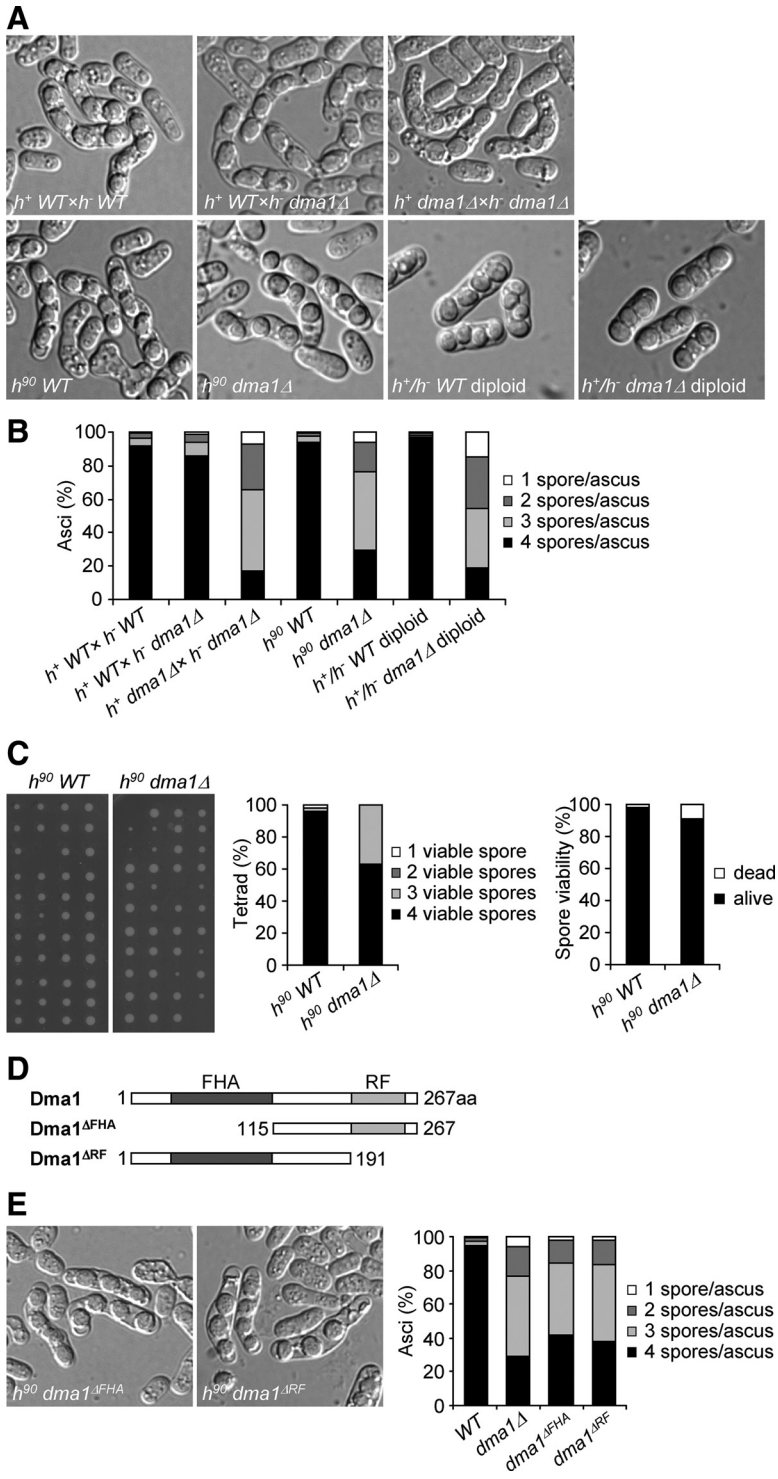

Figure 4. Dma1 is required for proper spore formation. (A and B) The *dma1*Δ mutants generate spore formation defects. The wild-type and *dma1*Δ strains were induced to enter meiosis on ME plates by heterothallic crosses ($h^+ \times h^-$), homothallic mating (h^{90}), or *pat1-114/pat1-114* diploid at 30°C or 34°C (for *pat1-114/pat1-114* diploid). (A) DIC images of the asci are shown. (B) Quantification of spore number per ascus. At least 300 tetranucleate cells containing at least one spore were counted for each sample. (C) Germination efficiency of wild-type and *dma1*Δ spores in homothallic (h^{90}) strains. Normal-looking four-spore asci formed on sporulating ME plates for 2 d were randomly chosen and grown on YES solid medium at 30°C after dissection using micromanipulator. Colonies formed after 3 d of incubation at 30°C were photographed and counted. Samples of dissected tetrads are shown (left). Tetrads fell into four categories depending on the spore number (from 1 to 4) were analyzed (middle) and the number of colonies grown up were counted (right) in 45 wild-type or 43 *dma1*Δ tetrads respectively. (D) Schematic representation of Dma1 structure. Full-length and partial deletion constructs with FHA or RF domains truncated are shown. (E) Spore formation defects in partial deletion mutants $Dma1^{\Delta FHA}$ or $Dma1^{\Delta RF}$. Homothallic h^{90} strains carrying genomic $dma1^{\Delta FHA}$ or $dma1^{\Delta RF}$ at original endogenous $dma1^+$ locus were induced into sporulation on ME plate at 30°C. At least 300 tetranucleate cells containing at least one spore were counted for each sample.

the assembly of the forespore membrane. While cells deleted for $spo3^+$ completely fail to form the forespore membrane (Nakamura *et al*., 2001), cells with GFP tagged Spo3 (Spo3-GFP) present only slightly compromised spore formation (Perez-Hidalgo *et al*., 2008; Yan *et al*., 2008). Through analysis of the *dma1*Δ cells carrying spo3-GFP, we found strong negative genetic interaction between *dma1*Δ and *spo3-GFP*, as we observed severe impairment in sporulation in these cells (Figure 7A). Similar to our observations with GFP-Psy1, we also found collapsed Spo3-GFP signals within cytoplasm in *dma1*Δ cells (Figure 7B), consistent with the idea that Dma1 is involved in maintaining the growth of FSM during sporulation. One major difference between the localization of Spo3-GFP and that of GFP-Psy1 in *dma1*Δ asci is that collapsed Spo3-GFP was frequently found away from nuclei, whereas aggregated GFP-Psy1 usually overlapped with or attached to nuclei (compare Figure 5B and Figure 7B). These results showed that re-

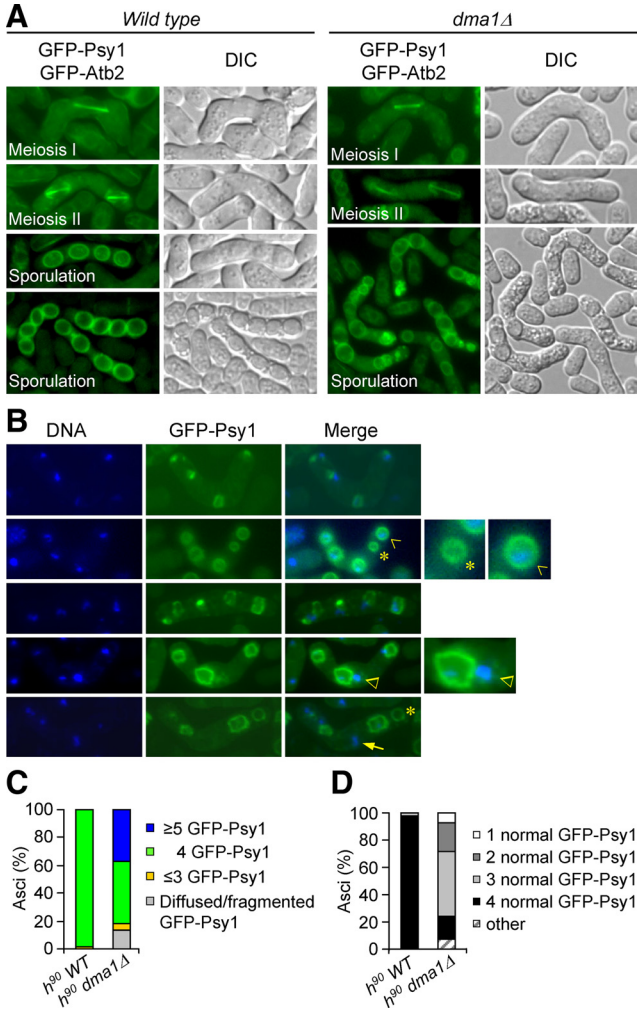

Figure 5. Spore membrane assembly is aberrant in *dma1*Δ cells. (A) Localization of GFP-Psy1 in wild-type and *dma1*Δ cells. Wild-type and *dma1*Δ cells simultaneously expressing both GFP-Psy1 and GFP-Atb2 were induced to undergo meiosis on ME plate at 30°C. Meiotic cells were visualized by fluorescence and DIC microscopes. Examples of cells at meiosis I, II, and sporulation are shown. Abnormal FSMs are observed frequently in *dma1*Δ asci. (B) Abnormal number and morphology of GFP-Psy1 and failed encapsulation of nuclei in *dma1*Δ cells. *dma1*Δ cells expressing only GFP-Psy1 were induced to undergo meiosis on ME plate at 30°C. Live meiotic cells were visualized by fluorescence microscope after Hoechst 33342 staining. Green panel reveals GFP-Psy1 localization, whereas the blue panel reveals the nuclei. An example of normal looking GFP-Psy1 sphere with properly enclosed nucleus is indicated by an open arrow. Several examples of abnormal GFP-Psy1 and failure of encapsulation of nuclei within spore membranes are shown: empty GFP-Psy1 sphere (asterisk); failed encapsulation of nucleus with diffused GFP-Psy1 (triangle); and completely mislocalized nucleus without connecting Psy1 materials (arrow). (C and D) Quantification of asci with abnormal number of GFP-Psy1 signals (C) and asci with normal-looking sphere-like GFP-Psy1 signals (D) in wild-type and *dma1*Δ cells.

duced Spo3 function strongly prevents proper engulfment of nuclei when *dma1*$^+$ is deleted.

Dma1 Functions in Parallel with SIN Signaling and Meiosis-Specific Kinase Slk1/Mug27 during Forespore Membrane Assembly

During mitotic exit and cytokinesis, Dma1 may act to antagonize SIN signaling by inhibiting the SPB localization of SIN components including the upstream SIN activator Plo1 kinase (Guertin *et al.*, 2002b). Recent studies have shown that the SIN components localize to the SPBs during meiosis and play an important positive role in forespore membrane assembly during sporulation (Krapp *et al.*, 2006). Because the sporulation defects we observed in *dma1*Δ cells are similar to those reported for SIN mutants, we wondered whether Dma1 and SIN proteins possibly perform overlapping functions in the regulation of sporulation. We constructed several homothallic double mutants between *dma1*Δ and temperature-sensitive SIN or SIN activator mutants, including the *sid4-A1*, *cdc11-123*, *spg1-106*, *cdc7-24*, *sid1-239*, *mob1-1*, *sid2-250* and *plo1-24C* mutants. Except for *dma1*Δ *sid4-A1* and *dma1*Δ *spg1-106*, which could not survive at 30°C and thus the analyses of these mutants were only carried out at 25°C, examination of sporulation in other mutants was performed at both permissive and semipermissive temperatures (25 and 30°C). Our results showed that spore formation defects observed in the *dma1*Δ single mutant were not significantly enhanced by most SIN mutations (Figure 8, A and B and Supplemental Figure S4). However, we observed that homothallic *dma1*Δ *spg1-106* and *dma1*Δ *mob1-1* cells were completely unable to sporulate under conditions in which single *spg1-106* or *mob1-1* mutants were not apparently compromised for sporulation (Figure 8, A and B), suggesting that Dma1 might function in parallel with Spg1 and Mob1 in sporulation. This result is quite similar to the previous observations that the spore formation is severely impaired in *slk1*Δ *spg1-106* and *slk1*Δ *mob1-R4* double mutants at permissive temperature, which allowed the deduction that the SIN and Slk1 function in parallel but not in the same pathway in spore formation (Perez-Hidalgo *et al.*, 2008; Yan *et al.*, 2008).

Recent studies have shown that a Sid2-related meiosis-specific kinase Slk1/Mug27 and SIN proteins perform overlapping functions in the regulation of sporulation in fission yeast (Perez-Hidalgo *et al.*, 2008; Yan *et al.*, 2008). Our studies on Dma1 strongly suggested it also regulates sporulation in an independent pathway from SIN signaling. We wondered whether Dma1 and Slk1 were also functionally overlapping in regulating sporulation. To test this, we constructed a homothallic double mutant *dma1*Δ *slk1*Δ and analyzed its spore formation efficiency. We found that the double mutant was completely unable to form spores, suggesting that Dma1 and Slk1 regulate sporulation in an independent manner (Figure 8, C and D). Thus, it seems likely there are at least three parallel signaling pathways involved in controlling proper sporulation in fission yeast (see Figure 9).

Quite unexpectedly, we noticed that Slk1-GFP signals in *dma1*Δ cells seemed brighter than those observed in wild-type cells (Fig. S5A). This observation was supported by our quantification of intensities of Slk1-GFP signals in both wild-type and *dma1*Δ cells (Supplemental Figure S5B). Furthermore, we found that deletion of *dma1*$^+$ caused elevated Slk1 protein level and delayed decay of Slk1 during meiosis II and sporulation when cells were synchronously induced into meiosis (Supplemental Figure S5C). These data suggested that brighter Slk1-GFP signals in *dma1*Δ cells were most likely derived from its higher protein level. Interestingly, we also found that the complexes immunoprecipitated by anti-GFP antibodies (recognizing Dma1-GFP) contained Slk1 (Supplemental Figure S5D), indicating that these two proteins are at least present in the same complex even if not directly interacting during certain period of meiosis. However, we failed to observe any aberrant sporulation or disrupted spore formation upon overexpression of Slk1 (Supplemental Figure S5E). Also, elevated level of Slk1 did not enhance or rescue sporulation defects in *dma1*Δ cells

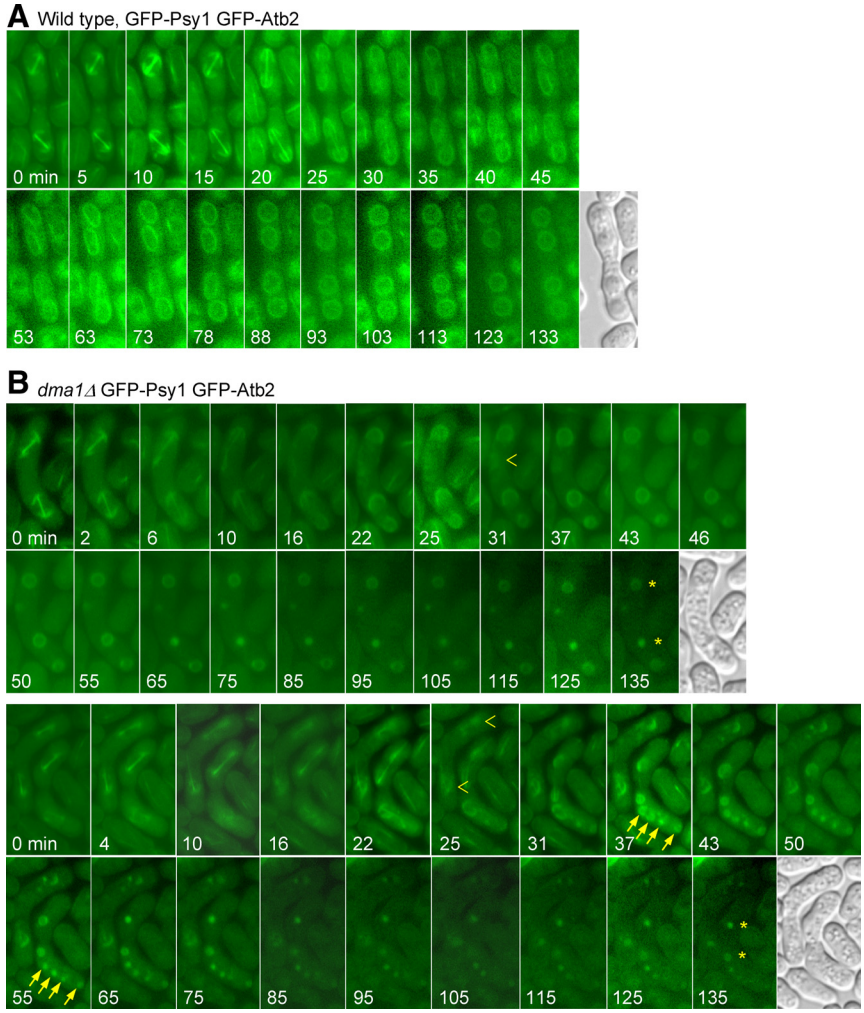

Figure 6. Time-lapse analysis of dynamic FSM formation in *dma1*Δ mutant. Homothallic wild-type (A) or *dma1*Δ (B) cells carrying GFP-Psy1 and GFP-Atb2 were first induced to enter meiosis as in Figure 5A, and then live images were captured. These images show a subset of GFP images captured every 3–10 min. Numbers indicate the time (in minutes) from the time point where the spindles were fully assembled at meiotic metaphase II. Asterisks denote the FSMs which were initially normal looking but subsequently became smaller or collapsed. Open arrows indicate the FSMs which were not properly developed into cup-like structures from the beginning. Arrows denote multiple GFP-Psy1–containing structures which could not develop into mature FSMs.

(Supplemental Figure S5E). Therefore, although an aberrant amount of Slk1 is retained as a consequence of *dma1*$^+$ deletion, simply overexpressing Slk1 alone does not mimic the *dma1*Δ defect in spore formation, suggesting that Dma1 may regulate levels of multiple proteins in addition to Slk1 during meiosis and sporulation.

DISCUSSION

It has been previously reported that Dma1, which resides at SPB after mitotic metaphase, functions as a negative regulator of mitotic exit and cytokinesis in late mitosis (Murone and Simanis, 1996; Guertin *et al*., 2002b). In the present study, we analyzed functions of *dma1*$^+$ in meiosis and sporulation. We found *dma1*$^+$ was transcriptionally induced during meiotic prophase and accumulated at meiosis I and II, during which time it localized to the SPB. Although cells lacking *dma1*$^+$ displayed minor chromosome segregation defects during meiosis, the majority of *dma1*Δ cells underwent meiosis I and II without obvious defects, instead these cells could not produce asci with the normal number of spores. These observations suggest that the inability of *dma1*Δ mutants to sporulate properly is unrelated to defects in progression through meiosis I and II and fidelity of nuclear division. Rather, our careful analyses of spore formation by following the localization and behavior of t-SNARE (syntaxin) Psy1 in *dma1*Δ cells revealed that the defect was due to inability to properly develop or maintain the FSM, and a similar observation was independently reported in a recent study (Krapp *et al*., 2010). These data suggested Dma1 is required for the proper formation of the FSM and/or assembly of the spore wall. This conclusion is further supported by our results in which *dma1*Δ cells carrying Spo3-GFP were completely unable to sporulate under conditions in which Spo3-GFP alone was only negligibly compromised for sporulation. We believe that the localization and function of untagged Spo3 protein is also defective when *dma1*$^+$ gene is deleted, because both Spo3 and Psy1 are involved in FSM assembly during sporulation, and previous studies have shown that Spo3 and Psy1 are functionally coupled and they affect each other's localization at FSM (Nakamura *et al*., 2001; Maeda *et al*., 2009). In a recent study, Simanis and colleagues also examined the localization of Meu14 which is localized at the leading edge of the FSM and found extra Meu14-GFP rings forming during FSM expansion in *dma1*Δ mutants (Krapp *et al*., 2010). This observation suggests the proper closure of FSM is also disregulated in the absence of *dma1*$^+$.

Recent studies have shown that SIN components are actively involved in spore formation (Krapp *et al*., 2006). The phenotype of *dma1*Δ in sporulation has strong similarity to what has been observed in SIN mutants, including distorted localization of Psy1, and this has been correlated with the

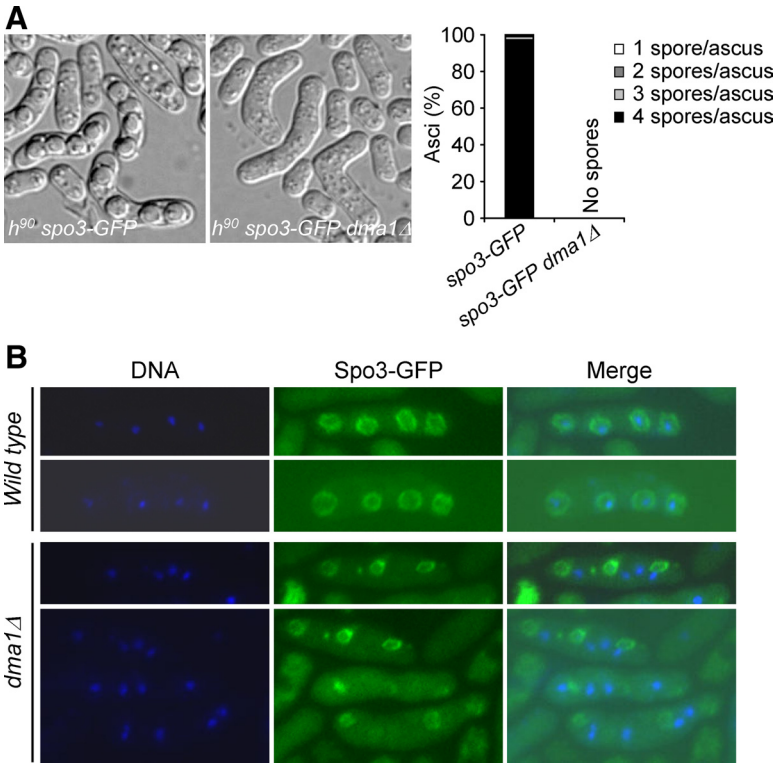

Figure 7. Negative genetic interaction between *spo3-GFP* and *dma1*Δ mutant. Homothallic wild-type and *dma1*Δ strains carrying *spo3*-GFP were induced into meiosis on ME plate at 30°C. (A) Spore formation efficiency was monitored by DIC microscope and quantified. (B) Nuclei and Spo3-GFP were visualized by fluorescence microscope after Hoechst 33342 staining.

cause for defective FSM extension and assembly in SIN mutants (Krapp *et al*., 2006). The disrupted localization of Psy1 in SIN and *dma1*Δ mutants is consistent with the assumption that the SIN signaling and Dma1 might fulfill their functions, at least in part, by controlling membrane and/or protein trafficking to the FSM during sporulation (Krapp *et al*., 2006 and this study). Therefore, our studies established a functional connection between Dma1 and the SIN signaling in regulating sporulation in fission yeast.

In this study, our detailed characterization on sporulation defects in *dma1*Δ mutant cells supports our conclusion that Dma1 positively regulates sporulation, similarly to the SIN and the meiosis-specific kinase Slk1/Mug27 (Krapp *et al*., 2006; Ohtaka *et al*., 2008; Perez-Hidalgo *et al*., 2008; Yan *et al*., 2008). This is surprising and rather different from the case during mitosis where Dma1 plays an antagonizing role on SIN signaling. Our genetic analyses in double mutants between *dma1*Δ and SIN mutations or *slk1*Δ suggested that

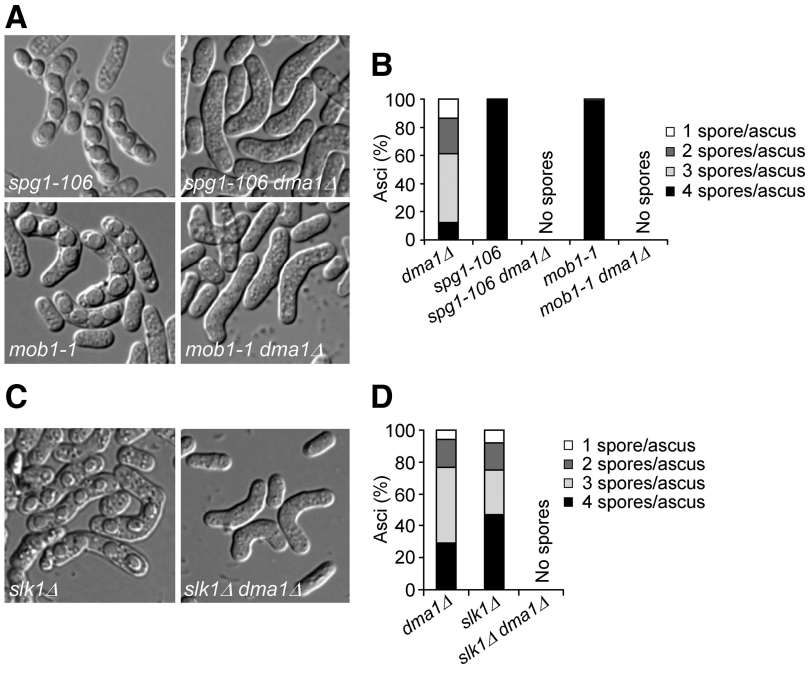

Figure 8. Negative genetic interactions between Dma1 and SIN signaling and Slk1 during forespore membrane assembly. (A and B) Synthetic genetic interactions between *dma1*Δ and two SIN mutants, *spg1-106* and *mob1-1*. Homothallic single SIN mutants and double mutants (*dma1*Δ *spg1-106* and *dma1*Δ *mob1-1*) were induced into meiosis on ME plate at 25°C for >20 h. Spore formation was monitored by DIC microscope (A) and spore formation efficiency was quantified (B). (C and D) Synthetic genetic interaction between *dma1*Δ and *slk1*Δ mutant. Homothallic single *slk1*Δ and double *dma1*Δ *slk1*Δ mutants were induced into meiosis on ME plate at 30°C. Spore formation was monitored by DIC microscope (C), and spore formation efficiency was quantified (D).

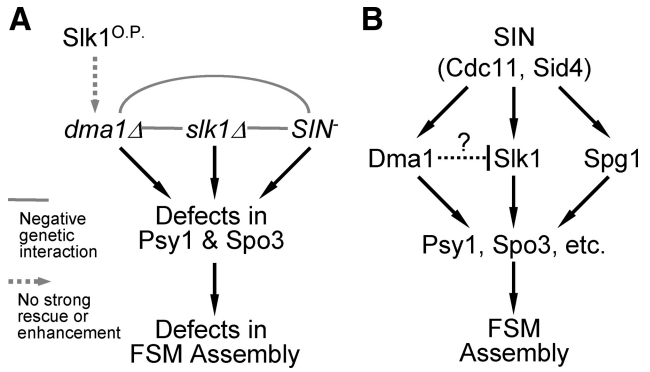

Figure 9. (A) Summary of the known genetic interactions and newly identified interactions in this study between *dma1*Δ, *slk1*Δ, and SIN mutations. No strong rescue or enhancement of overexpressed Slk1 (labeled as $Slk1^{O.P.}$) on sporulation defects in *dma1*Δ mutant is also indicated by dotted arrow. (B) Schematic representation of possible regulation of forespore membrane assembly in fission yeast. The proper assembly of forespore membrane during sporulation may require several signaling proteins, including SIN proteins, Slk1, and Dma1, to participate. Upstream SIN protein Spg1 synergizes with both Dma1 and Slk1.

Dma1, SIN, and Slk1 might work in parallel in regulating sporulation, and these pathways probably converge at regulating membrane and/or protein trafficking required for proper FSM development (Figure 9). However, the precise mechanisms linking Dma1, SIN, Slk1, and forespore membrane assembly is not fully understood, and it is not clear whether Dma1, SIN, and Slk1 carry out a common function during sporulation, or act through distinct mechanisms. Our observation that overexpression of *dma1*$^+$ in wild-type background during meiosis led to defective spore formation (data not shown) suggests that elevated level of Dma1 is detrimental to proper spore development. It also tells us that it is possible that the levels or activities of one or more proteins must be under precise control by Dma1 during meiosis, too much or too little of these proteins may cause defective sporulation. Consistent with our assumption that Dma1 may regulate several target proteins and have multiple roles in meiosis, Simanis and colleagues have recently shown that *dma1*Δ also displayed additive sporulation defects with septin mutant *spn5*Δ and leading edge protein mutant *meu14*Δ (Krapp *et al*., 2010).

One interesting, but puzzling, observation in our study was that *dma1*Δ only showed negative genetic interactions with a few SIN mutations (such as *spg1-106* and *mob1-1*) but not with other hypomorphic alleles tested. This is quite similar to observations in a previous study, in which *slk1*Δ only showed synthetic phenotypes with the same set of SIN mutants but not others (Yan *et al*., 2008). One obvious difference between *dma1*Δ and *slk1*Δ is that *slk1*Δ also completely lost ability to sporulate when function of Sid2 (the most downstream SIN component) was compromised (Perez-Hidalgo *et al*., 2008; Yan *et al*., 2008) while *dma1*Δ did not (our data in this study). So, if the genetic interaction between *slk1*Δ and upstream SIN mutant *spg1-106* could be interpreted as a direct consequence of reduced function of the downstream Sid2, this explanation could not be applied to *dma1*Δ. It is possible that Dma1 and Slk1 have distinct patterns of overlapping function with certain SIN proteins.

In mitosis, the recruitment of Dma1 to SPB is dependent on SIN scaffold protein Sid4 but not Cdc11 (Guertin *et al*., 2002b). During meiosis, although the initial recruitment of Dma1 to SPBs is not dependent on SIN proteins, its subsequent stable maintenance at SPBs at anaphase II clearly requires both Cdc11 and Sid4. Interestingly, our genetic analyses suggested that SPB-localized Dma1 has different functions during mitosis and meiosis. During mitosis Dma1 antagonizes the SIN, but during meiosis, Dma1 and the SIN appear to perform similar functions. It is currently unclear how Dma1 switches from its inhibitory role on SPB-localized SIN components during mitotic exit and cytokinesis to its positive effect on sporulation. Several possibilities may exist, for example, Dma1 may switch its binding or functional partners in mitosis and meiosis, or Dma1 is differently regulated during mitosis and meiosis. Search for mitosis- and meiosis-specific binding partners of Dma1 might be able to help us to clarify this issue more thoroughly.

The SPB plays two different roles during meiosis, one is for microtubule assembly and the other for construction of the FSM (reviewed in Shimoda, 2004). The latter function is accompanied by meiotic SPB modification. Although many SPB proteins develop a characteristic crescent shape during the late stages of meiosis as the outer plaque is remodeled to promote spore formation, the SPB-localized SIN proteins and Dma1 do not show this shape (Krapp *et al*., 2006 and this study). Moreover, neither SPB modification nor initiation of the FSM formation is apparently impaired when SIN signaling is compromised or when *dma1*$^+$ is absent (Krapp *et al*., 2006; Krapp *et al*., 2010; and this study). These observations suggest that both Dma1 and SIN proteins do not necessarily associate with the modified SPB in order to fulfill their functions in FSM development.

Similarly to Dma1, the meiosis-specific kinase Slk1/Mug27 has been shown to be positively required for sporulation in fission yeast (Ohtaka *et al*., 2008; Perez-Hidalgo *et al*., 2008; Yan *et al*., 2008; and this study). However, one puzzling observation in our study is that Slk1 is somehow negatively regulated by Dma1 and a similar result has been reported recently by others (Krapp *et al*., 2010). As compared with wild-type cells, we could detect stronger signals of Slk1-GFP at SPBs and elevated overall protein level in *dma1*Δ cells. Our result showing the coexistence of both Dma1 and Slk1 in a immunoprecipitated complex during meiosis suggests it is probably related to their functional connection. However, forced overexpression of Slk1 did not cause any obvious sporulation defects as observed in *dma1*Δ cells, so the elevated Slk1 level does not appear to be the direct cause of the sporulation defect in *dma1*Δ cells, and Dma1 may act through multiple partners in addition to Slk1. Alternatively, it is possible that in certain circumstances, Dma1 may negatively fine tune the signals from Slk1 for the process of FSM formation. Dma1 has long been considered to be a potential E3 ubiquitin ligase since its discovery (Murone and Simanis, 1996; Guertin *et al*., 2002b), as it contains a RING-H2 finger domain which is present in some confirmed E3 ubiquitin ligases. Whether the RING finger domain in Dma1 carries E3 ubiquitin ligase activity and whether this activity is directly required for its function in sporulation regulation are interesting questions for future studies to answer. Our observation that RING finger-deleted Dma1 cannot faithfully support sporulation is consistent with this possibility. If Dma1 indeed played roles in negatively regulating some proteins' level in sporulation through its potential ubiquitin E3 ligase activity, then the identification of candidate molecules will be an important direction for future studies.

ACKNOWLEDGMENTS

We gratefully acknowledge Drs. Mohan K. Balasubramanian, Ian Hagan, Sergio Moreno, Yoshinori Watanabe, Takashi Toda, Masamitsu Sato, and Yeast Genetic Resource Center Japan (YGRC) for generously providing yeast strains or plasmids and Dr. K. Gull for providing TAT1 antibodies. We thank Dr. Dannel McCollum for his advice on experiments and his critical reading and correction of the manuscript. We thank Zhen-wei Gao for his important initial contributions to this project, Drs. Viesturs Simanis and Andrea Krapp for sharing with us unpublished results, and Drs. Josef Loidl and Alexander Lorenz for their suggestions on diploid strain construction. We also thank two anonymous reviewers for their comments and suggestions on experiments. This work was supported by grants from the National Natural Science Foundation of China (No. 30771078, No. 30871376), Key Project of Chinese Ministry of Education (No. 108076), and the Natural Science Foundation of Fujian Province of China (No. 2007F3098) (to Q.W.J.). This work was also supported by grants from the Science Planning Program of Fujian Province (2009J1010) and by 111 Project (B06016).

REFERENCES

Arellano, M., Cartagena-Lirola, H., Nasser Hajibagheri, M. A., Duran, A., and Henar Valdivieso, M. (2000). Proper ascospore maturation requires the chs1+ chitin synthase gene in *Schizosaccharomyces pombe.* Mol. Microbiol. *35*, 79–89.

Bridge, A. J., Morphew, M., Bartlett, R., and Hagan, I. M. (1998). The fission yeast SPB component Cut12 links bipolar spindle formation to mitotic control. Genes Dev. *12*, 927–942.

Chang, L., and Gould, K. L. (2000). Sid4p is required to localize components of the septation initiation pathway to the spindle pole body in fission yeast. Proc. Natl. Acad. Sci. USA *97*, 5249–5254.

Guertin, D. A., Trautmann, S., and McCollum, D. (2002a). Cytokinesis in eukaryotes. Microbiol. Mol. Biol. Rev. *66*, 155–178.

Guertin, D. A., Venkatram, S., Gould, K. L., and McCollum, D. (2002b). Dma1 prevents mitotic exit and cytokinesis by inhibiting the septation initiation network (SIN). Dev. Cell. *3*, 779–790.

Hagan, I., and Yanagida, M. (1995). The product of the spindle formation gene sad1+ associates with the fission yeast spindle pole body and is essential for viability. J. Cell Biol. *129*, 1033–1047.

Hirata, A., and Shimoda, C. (1994). Structural modification of spindle pole bodies during meiosis II is essential for the normal formation of ascospores in *Schizosaccharomyces pombe*: ultrastructural analysis of spo mutants. Yeast *10*, 173–183.

Hochstenbach, F., Klis, F. M., van den Ende, H., van Donselaar, E., Peters, P. J., and Klausner, R. D. (1998). Identification of a putative alpha-glucan synthase essential for cell wall construction and morphogenesis in fission yeast. Proc. Natl. Acad. Sci. USA *95*, 9161–9166.

Iino, Y., and Yamamoto, M. (1985). Negative control for the initiation of meiosis in *Schizosaccharomyces pombe.* Proc. Natl. Acad. Sci. USA *82*, 2447–2451.

Ikemoto, S., Nakamura, T., Kubo, M., and Shimoda, C. (2000). *S. pombe* sporulation-specific coiled-coil protein Spo15p is localized to the spindle pole body and essential for its modification. J. Cell Sci. *113*, 545–554.

Kitajima, T. S., Miyazaki, Y., Yamamoto, M., and Watanabe, Y. (2003a). Rec8 cleavage by separase is required for meiotic nuclear divisions in fission yeast. EMBO J. *22*, 5643–5653.

Kitajima, T. S., Yokobayashi, S., Yamamoto, M., and Watanabe, Y. (2003b). Distinct cohesin complexes organize meiotic chromosome domains. Science *300*, 1152–1155.

Krapp, A., Collin, P., Cokoja, A., Dischinger, S., Cano, E., and Simanis, V. (2006). The *Schizosaccharomyces pombe* septation initiation network (SIN) is required for spore formation in meiosis. J. Cell Sci. *119*, 2882–2891.

Krapp, A., Del Rosario, E. C., and Simanis, V. (2010). The role of *Schizosaccharomyces pombe* dma1 in spore formation during meiosis. J. Cell Sci. *123*, 3284–3293.

Krapp, A., Schmidt, S., Cano, E., and Simanis, V. (2001). *S. pombe* cdc11p, together with sid4p, provides an anchor for septation initiation network proteins on the spindle pole body. Curr. Biol. *11*, 1559–1568.

Krapp, A., and Simanis, V. (2008). An overview of the fission yeast septation initiation network (SIN). Biochem. Soc. Trans. *36*, 411–415.

Liu, J., Tang, X., Wang, H., and Balasubramanian, M. (2000). Bgs2p, a 1,3-beta-glucan synthase subunit, is essential for maturation of ascospore wall in *Schizosaccharomyces pombe.* FEBS Lett. *478*, 105–108.

Loidl, J., and Lorenz, A. (2009). Analysis of *Schizosaccharomyces pombe* meiosis by nuclear spreading. Methods Mol. Biol. *558*, 15–36.

Maeda, Y., Kashiwazaki, J., Shimoda, C., and Nakamura, T. (2009). The *Schizosaccharomyces pombe* syntaxin 1 homolog, Psy1, is essential in the development of the forespore membrane. Biosci. Biotechnol. Biochem. *73*, 339–345.

Martin, V., Ribas, J. C., Carnero, E., Duran, A., and Sanchez, Y. (2000). bgs2+, a sporulation-specific glucan synthase homologue is required for proper ascospore wall maturation in fission yeast. Mol. Microbiol. *38*, 308–321.

Masai, H., Miyake, T., and Arai, K. (1995). hsk1+, a *Schizosaccharomyces pombe* gene related to *Saccharomyces cerevisiae* CDC7, is required for chromosomal replication. EMBO J. *14*, 3094–3104.

Mata, J., Lyne, R., Burns, G., and Bahler, J. (2002). The transcriptional program of meiosis and sporulation in fission yeast. Nat. Genet. *32*, 143–147.

McCollum, D., and Gould, K. L. (2001). Timing is everything: regulation of mitotic exit and cytokinesis by the MEN and SIN. Trends Cell Biol. *11*, 89–95.

Moreno, S., Klar, A., and Nurse, P. (1991). Molecular genetic analysis of fission yeast *Schizosaccharomyces pombe.* Methods Enzymol. *194*, 795–823.

Murone, M., and Simanis, V. (1996). The fission yeast dma1 gene is a component of the spindle assembly checkpoint, required to prevent septum formation and premature exit from mitosis if spindle function is compromised. EMBO J. *15*, 6605–6616.

Nakamura, T., Asakawa, H., Nakase, Y., Kashiwazaki, J., Hiraoka, Y., and Shimoda, C. (2008). Live observation of forespore membrane formation in fission yeast. Mol. Biol. Cell *19*, 3544–3553.

Nakamura, T., Nakamura-Kubo, M., Hirata, A., and Shimoda, C. (2001). The *Schizosaccharomyces pombe* spo3+ gene is required for assembly of the forespore membrane and genetically interacts with psy1(+)-encoding syntaxin-like protein. Mol. Biol. Cell *12*, 3955–3972.

Nakase, Y., Nakamura-Kubo, M., Ye, Y., Hirata, A., Shimoda, C., and Nakamura, T. (2008). Meiotic spindle pole bodies acquire the ability to assemble the spore plasma membrane by sequential recruitment of sporulation-specific components in fission yeast. Mol. Biol. Cell *19*, 2476–2487.

Ohtaka, A., Okuzaki, D., and Nojima, H. (2008). Mug27 is a meiosis-specific protein kinase that functions in fission yeast meiosis II and sporulation. J. Cell Sci. *121*, 1547–1558.

Ohtaka, A., Okuzaki, D., Saito, T. T., and Nojima, H. (2007a). Mcp4, a meiotic coiled-coil protein, plays a role in F-actin positioning during *Schizosaccharomyces pombe* meiosis. Eukaryot. Cell *6*, 971–983.

Ohtaka, A., Saito, T. T., Okuzaki, D., and Nojima, H. (2007b). Meiosis specific coiled-coil proteins in Shizosaccharomyces pombe. Cell Div. *2*, 14

Okuzaki, D., Satake, W., Hirata, A., and Nojima, H. (2003). Fission yeast meu14+ is required for proper nuclear division and accurate forespore membrane formation during meiosis II. J. Cell Sci. *116*, 2721–2735.

Perez-Hidalgo, L., Rozalen, A. E., Martin-Castellanos, C., and Moreno, S. (2008). Slk1 is a meiosis-specific Sid2-related kinase that coordinates meiotic nuclear division with growth of the forespore membrane. J. Cell Sci. *121*, 1383–1392.

Shimoda, C. (2004). Forespore membrane assembly in yeast: coordinating SPBs and membrane trafficking. J. Cell Sci. *117*, 389–396.

Tanaka, K., and Hirata, A. (1982). Ascospore development in the fission yeasts *Schizosaccharomyces pombe* and S. japonicus. J. Cell Sci. *56*, 263–279.

Vos, A., Dekker, N., Distel, B., Leunissen, J. A., and Hochstenbach, F. (2007). Role of the synthase domain of Ags1p in cell wall alpha-glucan biosynthesis in fission yeast. J. Biol. Chem. *282*, 18969–18979.

Yan, H., Ge, W., Chew, T. G., Chow, J. Y., McCollum, D., Neiman, A. M., and Balasubramanian, M. K. (2008). The meiosis-specific Sid2p-related protein Slk1p regulates forespore membrane assembly in fission yeast. Mol. Biol. Cell *19*, 3676–3690.